Article

Discovery Medicine 2024; 36(190): 2274–2286
https://doi.org/10.24976/Discov.Med.202436190.209

Angiotensin-converting Enzyme 2 Suppresses Pulmonary Fibrosis Associated with Wnt and TGF-β1 Signaling Pathways

Yanhua Tang[1,†], Ju Liu[1,†], Ling Liu[1,*]

[1]Rheumatology and Immunology Department, Jiujiang City Key Laboratory of Cell Therapy, The First Hospital of Jiujiang City, 332000 Jiujiang, Jiangxi, China

*Correspondence: liulingll85@163.com (Ling Liu)

[†]These authors contributed equally.

Published: 20 November 2024

Background: Pulmonary fibrosis is a severe respiratory condition marked by the formation of scar tissue in the lungs, which makes it distinguishable from atypical fibrosis. The specific mechanisms of angiotensin-converting enzyme 2 (ACE2) in pulmonary fibrosis are still unclear, although it has been demonstrated to have a significant role in this condition. The objective of this study was to examine the impact of ACE2 on lung fibrosis.

Methods: Both *in vivo* and *in vitro* experimental approaches were employed in this study to evaluate the function of ACE2. In the *in vivo* experiments, an animal model of pulmonary fibrosis was established by injecting 0.1 mL of bleomycin solution into C57BL/6 male mice, and the effects of ACE2 overexpression on pulmonary fibrosis were observed, for the animal group overexpressing ACE2 (Model+ACE2 group), treatments with SB505124 (transforming growth factor-β type I receptor (TGF-βRI) (ALK5) inhibitor) and XAV939 (Wnt Family Member 3a (Wnt3a) inhibitor) were administered, to evaluate the effects of these pathway inhibitors on ACE2 overexpression in the treatment of pulmonary fibrosis. Lung tissue samples were collected from the animals and subjected to pathological examination (hematoxylin and eosin (HE) and Masson's trichrome staining) to assess the degree of pathological inflammation and fibrosis. Concurrently, the expression levels of proteins and genes related to the ACE2, Wnt/glycogen synthase kinase (GSK)-3β/β-catenin, and TGF-β1/Smad2 signaling pathways were measured using Western blotting and quantitative reverse-transcription polymerase chain reaction (qRT-PCR) techniques. In the *in vitro* experiments, pulmonary fibrosis was simulated in human lung fibroblasts (HLFs), which were stimulated with TGF-β1. The correlation of ACE2 overexpression to attenuate pulmonary fibrosis with Wnt/GSK-3β/β-catenin and TGF-β1/Smad2 signaling pathways was explored.

Results: The ACE2 overexpression could effectively reduce pulmonary fibrosis and inflammation in mice and HLFs by modulating signaling pathways ($p < 0.01$). In mice, ACE2 reduced inflammation and collagen accumulation, decreasing levels of α-smooth muscle actin (α-SMA) and fibronectin ($p < 0.01$). Compared to the Model+ACE2 group, the Model+ACE2+SB505124 underwent a greater reduction in inflammation and fibrosis, as well as decreased levels of α-SMA and fibronectin ($p < 0.05$). Overexpression of ACE2, XAV939, and SB505124 all significantly reduced the expression levels of Wnt3a, β-catenin, p-GSK-3β, TGF-β1, and p-Smad2 proteins in mice with pulmonary fibrosis ($p < 0.05$). In HLFs, ACE2 counteracted TGF-β1 effects, reducing cell proliferation and levels of fibrosis markers such as collagen, α-SMA and fibronectin ($p < 0.01$). It also inhibited the TGF-β1-induced epithelial-mesenchymal transition (EMT), showcasing its therapeutic potential against lung fibrosis and inflammation by regulating key signaling pathways and EMT processes ($p < 0.01$).

Conclusion: The desirable effects of ACE2 in alleviating pulmonary fibrosis are associated with the regulation of the Wnt/GSK-3β/β-catenin and TGF-β1/Smad2 signaling pathway. These results offer significant evidence for further investigation into the potential use of ACE2 in treating pulmonary fibrosis and provide new avenues for the advancement of innovative therapeutic approaches.

Keywords: ACE2; pulmonary fibrosis; Wnt/GSK-3β/β-catenin; TGF-β1/Smad2/3; EMT

Introduction

Pulmonary fibrosis is a severe respiratory condition resulting in a substantial decline in lung function due to an overgrowth of fibrotic tissue that replaces healthy lung tissue [1–3]. This complex disease involves multiple molecular signaling pathways [4,5]. Previous studies have indicated that the Wnt/glycogen synthase kinase (GSK)-3β/β-catenin and transforming growth factor-β1 (TGF-β1)/Smad2 signaling pathways have significant involvement in the onset and progression of pulmonary fibrosis [6–9]. Nonetheless, it remains unclear whether and how these two signaling pathways contribute to the impact of angiotensin-converting enzyme 2 (ACE2) on fibrosis. Furthermore, although previous research has indicated that ACE2 can alleviate pulmonary fibrosis, its precise mechanisms of action and potential therapeutic effects require further investigations [10].

Pulmonary fibrosis is a severe, progressive lung disease characterized by the scarring of lung tissue, leading to respiratory failure, substantial morbidity, and high mortality. Current treatment options are limited and primarily focus on symptom management rather than addressing the root cause of fibrosis. Thus, there is a pressing need for novel therapeutic strategies that can effectively target the underlying mechanisms of the disease. ACE2 has emerged as a promising therapeutic target due to its regulatory role in key signaling pathways involved in fibrosis. ACE2 has recently gained considerable attention [11,12]. It is a membrane protein enzyme widely distributed in various tissues and organs, including lung tissue [13]. Research has shown that ACE2 has a vital controlling function in the development of pulmonary fibrosis [14,15]. According to reports, ACE2 can attenuate the intensity of pulmonary fibrosis by obstructing the TGF-β1/Smad2/3 signaling pathway [16]. These studies provide important clues for understanding how ACE2 combats pulmonary fibrosis by modulating these two signaling pathways [17,18]. Nevertheless, the findings of these studies often vary and even conflict with each other, requiring additional investigations to address the discrepancies. By comprehensively understanding how ACE2 modulates the Wnt/GSK-3β/β-catenin and TGF-β1/Smad2/3 pathways, we can identify new intervention avenues for treating pulmonary fibrosis.

Although previous research has suggested that ACE2 can mitigate pulmonary fibrosis by regulating the TGF-β1/Smad2 signaling pathway, the precise interaction between the Wnt/GSK-3β/β-catenin and TGF-β1/Smad2 pathways and the specific mechanism by which ACE2 regulates these pathways to counteract pulmonary fibrosis remains uncertain. Furthermore, few studies have concurrently examined the impact of ACE2 on pulmonary fibrosis in both *in vivo* and *in vitro* experimental settings. Exploring these aspects will offer a broader understanding of the development of pulmonary fibrosis and enable the discovery of novel treatment strategies [19].

The objective of this research is to investigate the potential of ACE2 in mitigating pulmonary fibrosis through the concurrent regulation of the Wnt/GSK-3β/β-catenin and TGF-β1/Smad2/3 signaling pathways in both *in vivo* and *in vitro* environments. To elucidate the effects of ACE2 expression and activity on these two signaling pathways and their interplay, we employed an animal model and a cellular model of pulmonary fibrosis. Additionally, we assessed whether ACE2 ameliorates the severity of pulmonary fibrosis by modulating these pathways. By undertaking this study, we aim to uncover the underlying mechanisms by which ACE2 exerts its effects on pulmonary fibrosis and propose innovative therapeutic strategies. The clinical value of this research lies in its potential to develop ACE2-based therapies that offer more effective and targeted treatment options for patients diagnosed with this debilitating condition. This study not only aims to enhance our understanding of the molecular mechanisms driving pulmonary fibrosis but also seeks to pave the way for innovative clinical applications that could significantly improve patient outcomes.

Materials and Methods

Establishing Animal Model of Pulmonary Fibrosis

Thirty SPF-grade C57BL/6 male mice with an average weight of 20 $\pm$ 2 g were obtained from Beijing Charles River Company (Beijing, China; Experimental Animal Production License Number: 20170930A). The mice were divided into five groups: control group, Model+NC group, Model+ACE2 group, Model+ACE2+SB505124 group (transforming growth factor-β type I receptor (TGF-βRI) [ALK5] inhibitor SB-505124; 1 µM; Sigma, St. Louis, MO, USA), and Model+ACE2+XAV939 group (Wnt Family Member 3a (Wnt3a) inhibitor XAV939; 1 µM; Sigma). The mice were anesthetized by intraperitoneal injection of pentobarbital sodium (30 mg/kg, 21642-83-1, Shandong Xiya Chemical Industry Co., Ltd., Linyi, China), and their neck skin was sterilized using iodine and alcohol. The skin on the neck was cut, and the tissue in the front of the neck was cautiously separated (to prevent bleeding) to expose the trachea. In the control group, 0.1 mL of saline was administered through the trachea, while in the experimental groups, 0.1 mL of bleomycin (ST1450, 20 mg; Beyotime, Shanghai, China) dissolved in saline (5 mg/kg) was administered through the trachea. After injection, the mice were quickly inverted and rotated to ensure even distribution of bleomycin or saline in the lung tissue. Following the surgical procedure, the mice were provided with warmth and given time to recuperate before resuming regular food and water intake. Seven days after the bleomycin injection, the mice were treated with either ACE2 overexpression lentivirus transfection complex (cytomegalovirus (CMV) promoter, 25 ng/mL) or blank overexpression lentivirus transfection complex (CMV promoter, #V009680, Novo-

Pro, Shanghai, China), which was administered once every three days. The model mice that overexpressed ACE2 were categorized under the Model+ACE2 group. The mice in the Model+ACE2+SB505124 group and the Model+ACE2+XAV939 group were the Model+ACE2 mice that were intraperitoneally injected with SB505124 (2 mg/kg) and XAV939 (2 mg/kg), respectively, once every three days. The mice were euthanized after 9 days of treatment. Euthanasia was performed by intraperitoneal injection of pentobarbital sodium (3%, 150 mg/kg), and their lung tissues were collected for Masson's trichrome staining (for collagen) and immunohistochemical analysis.

Hematoxylin and Eosin Staining

The lung tissue specimens were dehydrated using varying concentrations of ethanol, cleared, embedded in paraffin, and then sliced into sections that were 4 µm in thickness. Deparaffinization was performed with water, followed by hematoxylin and eosin (HE) staining using a kit (C0105M, Beyotime, Shanghai, China). After staining, the tissue sections were dehydrated, and the slides were sealed using neutral gum. The prepared slides were examined under a microscope (DM5000, Leica Microsystems, Wetzlar, Germany) to detect any pathological alterations in the lung tissue. ImageJ (version 1.5f, National Institutes of Health, Bethesda, MD, USA) was used to measure the fiber areas of the HE-stained tissue sections.

Masson's Trichrome Staining

The left lung from each animal was fixed in polyformaldehyde for 12 hours, followed by rinsing with tap water. The tissue was soaked in 70% ethanol for 24 hours, then in 80%, 90%, and 100% ethanol for 3 hours each. Xylene was used for clearing for 20 minutes, followed by immersion in liquid paraffin for 3 hours and embedding. Upon reaching ambient temperature after cooling, the wax-embedded tissue was sliced at a 4 µm thickness, dried at a temperature of 37 °C, and then subjected to a 30-minute dewaxing process in xylene. The sections were then immersed in 100%, 90%, 80%, and 70% ethanol, followed by staining with Masson's collagen staining reagent (G1340, Solarbio, Beijing, China). The sections were dehydrated in 90% ethanol, immersed in xylene for 5 minutes, and sealed with neutral resin. The level of collagen accumulation in lung tissue was observed and assessed using a microscope. The Szapiel pathological evaluation method was applied to categorize fibrosis based on scores: 0 for no fibrosis, 1 for mild fibrosis (lesion range $\leq$20% of lung), 2 for moderate fibrosis (lesion range 20–50% of lung), and 3 for severe fibrosis (lesion range $\geq$50% of lung) with structural changes [3].

Table 1. Sequences of primers were utilized in this study.

Primer's name	Primer sequences (5′–3′)
Mouse-*α-Sma*-F	TTCAATGTCCCAGCCATGTA
Mouse-*α-Sma*-R	GAAGGAATAGCCACGCTCAG
Mouse-*Col-I*-F	GAGAGGTGAACAAGGTCCCG
Mouse-*Col-I*-R	AAACCTCTCTCGCCTCTTGC
Mouse-*Col-III*-F	GATCAGGCCAGTGGAAATGT
Mouse-*Col-III*-R	GTGTGTTTCGTGCAACCATC
Mouse-Fibronectin-F	ATGAGAAGCCTGGATCCCCT
Mouse-Fibronectin-R	GGAAGGGTAACCAGTTGGGG
Mouse-*Ace2*-F	GGTCCAGCAGCTTGTTTACTG
Mouse-*Ace2*-R	TTGAACTTGGGTTGGGCACT
Mouse-Vimentin-F	TGAGATCGCCACCTACAGGA
Mouse-Vimentin-R	TTGCGCTCCTGAAAAACTGC
Mouse-E-cadherin-F	CTTAGGTGCATGCCATAGTGG
Mouse-E-cadherin-R	TAGCTACCATCAAGAGCAGGC
Mouse-N-cadherin-F	CCGGAGATGGAGGAGATGA
Mouse-N-cadherin-R	TCCAGGTCAGTGGTGTCCAT
Mouse-*β*-actin-F	AGGGAAATCGTGCTGACATCAAA
Mouse-*β*-actin-R	ACTCATCGTACTCCTGCTTGCTGA
Homo-*α-SMA*-F	GATGGTGGGAATGGGACAAA
Homo-*α-SMA*-R	GCCATGTTCTATCGGGTACTTC
Homo-*COL-I*-F	GACATCCTGGTACGGTTGGA
Homo-*COL-I*-R	TCTGAGAGAAGGTGCTGAGC
Homo-*COL-III*-F	AATCAGGTAGACCCGGACGA
Homo-*COL-III*-R	CTCCTGGGATGCCATTTGGT
Homo-Fibronectin-F	CATCACAGTAGTTGCGGCAG
Homo-Fibronectin-R	CCCGTTTGTTGTGTCAGTGT
Homo-*ACE2*-F	CATTGGAGCAAGTGTTGGATCTT
Homo-*ACE2*-R	GAGCTAATGCATGCCATTCTCA
Homo-Vimentin-F	GAGTCCACTGAGTACCGGAG
Homo-Vimentin-R	ACGAGCCATTTCCTCCTTCA
Homo-E-cadherin-F	TTTGAAGATTGCACCGGTCG
Homo-E-cadherin-R	CAGCGTGACTTTGGTGGAAA
Homo-N-cadherin-F	GTGCCATTAGCCAAGGGAATTCAGC
Homo-N-cadherin-R	GCGTTCCTGTTCCACTCATAGGAGG
Homo-*β*-actin-F	CATCCGCAAAGACCTGTACG
Homo-*β*-actin-R	CCTGCTTGCTGATCCACATC

SMA, smooth muscle actin; *Col*, collagen; *Ace2*, angiotensin-converting enzyme 2.

Quantitative Reverse-Transcription Polymerase Chain Reaction (qRT-PCR)

Total RNA was extracted using TRIzol reagent (Catalog No: 15596026, Thermo Fisher Scientific, Waltham, MA, USA) following the manufacturer's instructions. The TaKaRa RNA PCR kit (Avian Myeloblastosis Virus, (AMV)) Ver.3.0 (RR019A, TaKaRa Bio Inc., Kafu City, Yamanashi Prefecture, Japan) was employed for performing reverse transcription reactions as per the manufacturer's guidelines. Briefly, RNA samples were reverse-transcribed into cDNA using the AMV reverse transcriptase provided in the kit. Primers specific to the target genes were synthesized by Dalian Baosheng Biotech Company (Dalian,

China). Quantitative polymerase chain reactions were performed using the synthesized cDNA as a template. The reaction conditions included an initial denaturation step at 94 °C for 60 seconds, followed by 30 cycles of denaturation at 94 °C for 60 seconds, annealing at 51 °C for 60 seconds, and extension at 72 °C for 90 seconds. The relative changes in mRNA expression within each experimental group were determined by calculating the ratio of the target gene to an internal reference. The sequences included in this study are shown in Table 1. The relative expression levels of mRNA were calculated using the $2^{-\Delta\Delta CT}$ method.

Western Blotting

Lung tissue specimens from each animal group were homogenized in Radioimmunoprecipitation assay (RIPA) lysis buffer (Catalog No: R0010, Solarbio, Beijing, China) supplemented with a protease inhibitor mixed in a ratio of 50:1. Tissue and cell proteins were extracted from the homogenized samples. The concentration of extracted proteins was determined using the BCA method (Catalog No: PC0020, Solarbio, Beijing, China). Protein samples were denatured for sodium dodecyl-sulfate polyacrylamide gel electrophoresis (SDS-PAGE), which was performed to separate proteins based on their molecular weight. Separated proteins were transferred from the gel to polyvinylidene difluoride (PVDF) membranes. The membranes were blocked with 5% low-fat milk at room temperature for 1 hour to prevent nonspecific binding. Antibodies against specific proteins were used: TGF-β1 (1:1000, ab215715, Abcam, Cambridge, UK), Wnt3a (1:1000, ab219412, Abcam, Cambridge, UK), β-catenin (1:1000, ab32572, Abcam, Cambridge, UK), phosphorylated GSK-3β (1:1000, ab141070, Abcam, Cambridge, UK), GSK-3β (1:1000, ab93926, Abcam, Cambridge, UK), phosphorylated Smad2 (1:1000, ab272332, Abcam, Cambridge, UK), Smad2 (1:1000, ab202445, Abcam, Cambridge, UK), glyceraldehyde 3-phosphate dehydrogenase (GAPDH) (1:1000, ab9485, Abcam, Cambridge, UK), β-actin (1:2000, ab8227, Abcam, Cambridge, UK), α-smooth muscle actin (α-SMA) (197240; Abcam, Cambridge, UK), and fibronectin (1:1000, ab2413, Abcam, Cambridge, UK). The membranes were incubated with respective antibodies overnight at 4 °C. Afterward, they were washed to remove excess antibodies. The membranes were then incubated with HRP-conjugated goat anti-rabbit immunoglobulin G (IgG) antibody (1:1000, ab6721, Abcam, Cambridge, UK) at room temperature for one hour. Subsequently, the membranes were exposed to an ECL exposure solution, and the protein bands were captured using an imaging system (ChemiDoc™ MP Imaging System, Bio-Rad, Hercules, CA, USA). The intensities of protein bands were analyzed using ImageJ software (version 1.5f, National Institutes of Health, Bethesda, MD, USA).

Human Lung Fibroblast Culture

Human lung fibroblasts (HLFs) (CL-0106, Pricella, Wuhan, China) were cultured in a 5% CO_2 incubator set at 37 °C. The culture medium used was composed of high-glucose dulbecco's modified eagle medium (DMEM) (iCell-0001, Cellverse Bioscience Technology, Shanghai, China) supplemented with 10% fetal bovine serum (FBS; Gibco) and 0.5% penicillin-streptomycin solution. Prior to utilization in this study, the cells had been subjected to mycoplasma detection and short tandem repeat (STR) identification. The cultured cells were grouped as follows: control group (treated with saline), TGF-β1 group (stimulated to induce TGF-β1), and TGF-β1+ACE2 group (stimulated to induce TGF-β1 and ACE2 overexpression).

Cell Transfection

HLFs were routinely passaged and obtained through the process of centrifugation. A total of 6×10^5 cells (in a 2 mL cell suspension) were seeded into each well of a 6-well plate, which was then incubated at 37 °C in an incubator with 5% CO_2 for 24 hours to promote cell adhesion.

In the transfection experiment, the empty plasmid was used as a negative control. ACE2 overexpression lentivirus transfection complex (CMV promoter, 25 ng/mL) or blank overexpression lentivirus transfection complex (CMV promoter) was transfected using the Lipofectamine 3000 kit (L3000001, Thermo Fisher Scientific, Waltham, MA, USA). After being incubated in the cell culture incubator for 6 to 8 hours, the culture medium was replaced with a fresh one, prior to incubating the cells in the cell culture incubator for 48 hours. Real-time PCR was employed to quantitatively analyze the transfection efficiency.

Cell Proliferation Assay Using Cell Counting Kit-8 (CCK-8)

HLFs were incubated in 96-well plates for a duration of 24 hours. Each group of the cellular model was tested in six duplicate wells. Following a 24-hour exposure to TGF-β1 at 10 ng/mL and 48 hours of transfection, the cells were supplemented with CCK-8 reagent (CA1210, Solarbio, Beijing, China), which had been diluted 10-fold in a complete culture medium. Three blank control groups were set up for this experiment. Following a 4-hour incubation period, a multifunctional microplate reader (BioTek Epoch Microplate Spectrophotometer, BioTek Instruments, Inc., Winooski, VT, USA) was utilized to measure the absorbance value at a wavelength of 460 nm.

Immunofluorescence

The HLFs were treated with 4% paraformaldehyde (P1110, Solarbio, Beijing, China) diluted in a solution of phosphate buffer saline (PBS) (P1022, Solarbio, Beijing, China) at room temperature. After that, they were incubated in 0.1% Triton X-100 (T8200, Solarbio, Beijing, China) diluted in a solution of PBS. Following two washes with Tris-

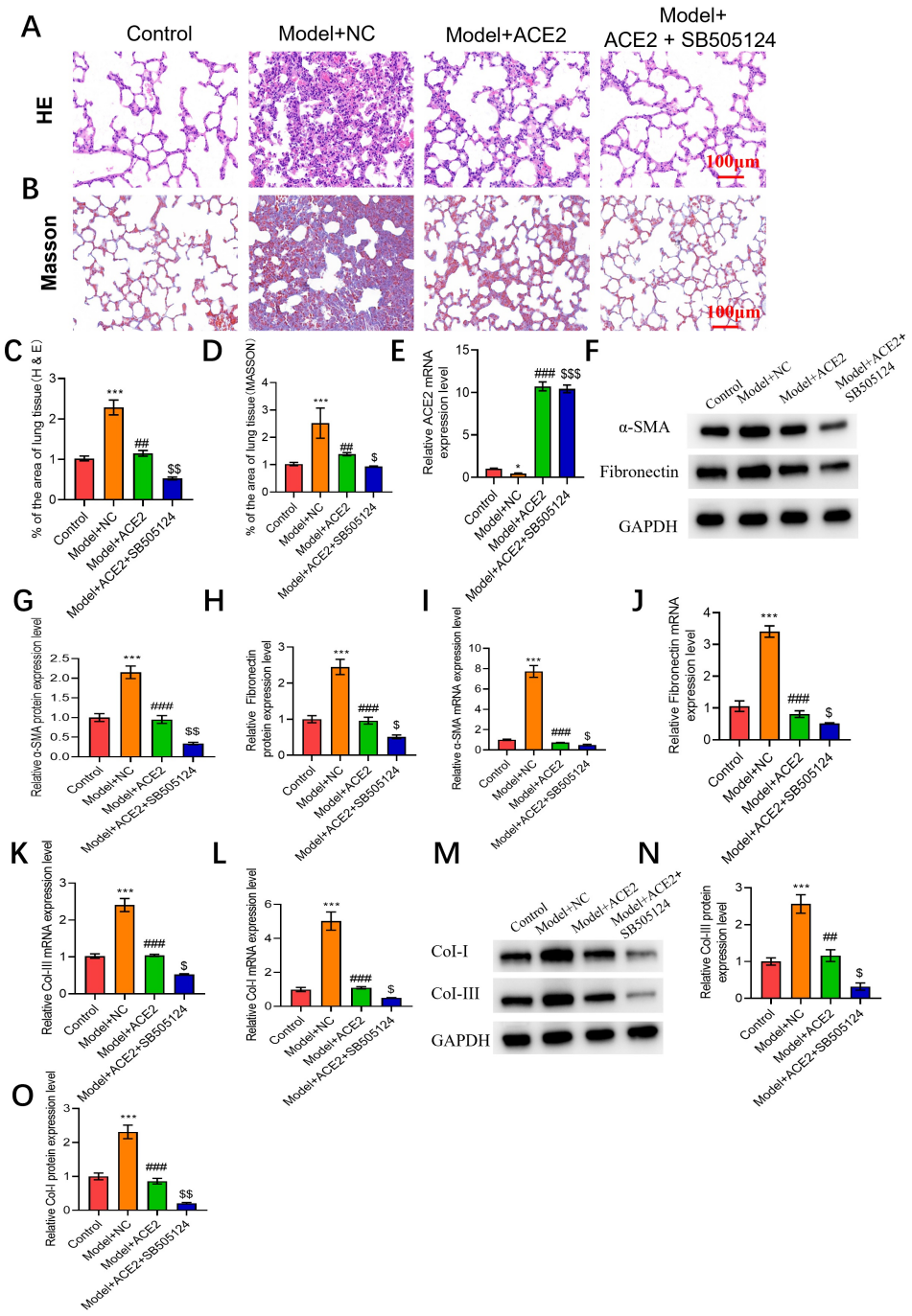

Fig. 1. Alterations in lung tissue of mice following angiotensin-converting enzyme 2 (ACE2) overexpression. (A,C) Evaluation of lung tissue architecture and inflammatory reaction in mice following hematoxylin and eosin (HE) staining. Scale bar: 100 μm. (B,D) Assessment of collagen accumulation in lung tissue following treatment using Masson's trichrome staining. (E) mRNA expression levels of *ACE2* in lung tissue of mice. (F–J) Protein and mRNA levels of α-smooth muscle actin (α-*SMA*) and fibronectin were analyzed using Western blotting and qRT-PCR. (K–O) Measurement of the protein and mRNA expression of collagen I (*Col-I*) and collagen III (*Col-III*) using Western blotting and qRT-PCR. n = 6, $^{*}p < 0.05$, $^{***}p < 0.001$ compared to control group; $^{\#\#}p < 0.01$, $^{\#\#\#}p < 0.001$ compared to Model+NC group; $^{\$}p < 0.05$, $^{\$\$}p < 0.01$, $^{\$\$\$}p < 0.001$ compared to Model+ACE2 group. qRT-PCR, quantitative reverse-transcription polymerase chain reaction; GAPDH, glyceraldehyde 3-phosphate dehydrogenase; HE, hematoxylin and eosin.

HCl buffer (T1010, Solarbio, Beijing, China), 100 μL of 5% goat serum was added for incubation at ambient temperature for 5 minutes. Following two washes with Tris-HCl buffer, the cells were incubated in 100 μL of anti-vimentin antibody solution (1:200, ab92547, Abcam, Cambridge, MA, USA) at 4 °C overnight. Subsequent to three

washes with Tris-HCl buffer, the cells were subjected to incubation in 100 µL of AlexaFluor 488-conjugated goat anti-rabbit immunoglobulin G (IgG) antibody solution (1:100, ab302644, Abcam, Cambridge, MA, USA) at ambient temperature for a duration of 30 minutes. After washing, the cells were mounted using a mounting medium that included 4′,6-Diamidino-2′-phenylindole (DAPI). Images were captured using a confocal fluorescence microscope (TiE2000, Nikon, Tokyo, Japan).

Statistical Analysis

The analysis of data was conducted using SPSS 20.0 (IBM, Armonk, NY, USA). The data are expressed as mean ± standard deviation. Intergroup comparisons were conducted using one-way analysis of variance (ANOVA), followed by pairwise comparisons using the least significant difference (LSD) post-hoc test. A p-value below 0.05 was considered statistically significant.

Results

Pathological Changes in Lung Tissue of Mice after ACE2 Overexpression

To observe structural alterations and inflammatory reactions, we performed histological analysis on mouse lung tissue by means of HE staining and Masson's trichrome staining (Fig. 1A–D). The results showed that, compared to the control group, the Model+NC group had significantly higher levels of inflammation and fibrosis ($p < 0.001$). Compared to the Model+NC group, the Model+ACE2 group exhibited significantly reduced inflammation and fibrosis levels ($p < 0.01$). The inflammation and fibrosis levels in the Model+ACE2+SB505124 group were significantly lower than those in the Model+ACE2 group ($p < 0.01$ and $p < 0.05$, respectively). The mRNA expression efficiency of *ACE2* was significantly higher in the Model+ACE2 group and the Model+ACE2+SB505124 group than in the control group and the Model+NC group ($p < 0.001$) (Fig. 1E). Next, we evaluated the changes in protein and mRNA expression levels of α-*SMA*, fibronectin, collagen I (*Col-I*), and collagen III (*Col-III*) in following ACE2 overexpression. The results indicated that, compared to the control group, the Model+NC group had significantly elevated protein and mRNA levels of α-*SMA*, fibronectin, *Col-I*, and *Col-III* ($p < 0.001$) (Fig. 1F–O). In the Model+ACE2 group, the protein and mRNA levels of α-*SMA*, fibronectin, *Col-I*, and *Col-III* were significantly lower than those in the Model+NC group ($p < 0.001$ and $p < 0.01$, respectively). Compared to the Model+ACE2 group, the Model+ACE2+SB505124 group had even lower protein and mRNA levels of α-*SMA*, fibronectin, *Col-I*, and *Col-III* ($p < 0.01$ and $p < 0.05$, respectively).

ACE2-Mediated Suppression of Pulmonary Fibrosis Associated with Wnt3a/β-Catenin and TGF-β1/Smad2 Signaling Pathways

Western blotting was performed to analyze the protein levels related to the Wnt3a/β-catenin and TGF-β1/Smad2 signaling pathways. According to the findings, compared to the control group, the Model group showed significantly increased protein levels of Wnt3a and β-catenin, as well as elevated expression of p-GSK-3β/GSK-3β. However, in the Model+ACE2 group and the Model ACE2+XAV939 (Wnt3a inhibitor) group, the protein levels of Wnt3a, β-catenin, and p-GSK-3β/GSK-3β were significantly decreased ($p < 0.001$) (Fig. 2A–D). Besides that, we also found that the expression of TGF-β1 and p-Smad/Smad2 was significantly increased in the Model group, but reduced in the Model+ACE2 group and the Model+ACE2+SB505124 (TGF-β1 inhibitor) group ($p < 0.001$, $p < 0.01$, and $p < 0.05$, respectively) (Fig. 2E–G).

Protective Effects of ACE2 Overexpression against the Damage Induced by TGF-β1 in Human Fetal Lung Fibroblasts

The investigation focused on examining the effect of ACE2 overexpression on HLFs treated with TGF-β1. The Model+ACE2 group exhibited a higher expression level of ACE2 in comparison to the control group, suggesting the successful overexpression of the *ACE2* gene ($p < 0.001$) (Fig. 3A). The CCK-8 assay demonstrated that the cell proliferation rate of HLFs was elevated in the TGF-β1 group in comparison to the control group ($p < 0.01$). Nonetheless, the TGF-β1+ACE2 group exhibited a reduced cell proliferation rate compared to the TGF-β1 group ($p < 0.01$) (Fig. 3B). Afterward, the mRNA levels of *Col-I*, *Col-III*, α-*SMA*, and fibronectin were assessed in HLFs. In the TGF-β1group, the levels of Col-I, Col-III, α-SMA, and fibronectin were found to be the most elevated ($p < 0.001$ and $p < 0.01$, respectively). Nevertheless, in the TGF-β1+ACE2 group, the levels of these markers were reduced compared to the group treated with TGF-β1 alone ($p < 0.001$ and $p < 0.01$, respectively) (Fig. 3C–F). This indicates that increased ACE2 expression may mitigate the production of collagen and fibronectin induced by TGF-β1, consequently decreasing the extent of pulmonary fibrosis. We also found that the expression of α-SMA and fibronectin levels was elevated in the TGF-β1 group in comparison to the control group ($p < 0.001$ and $p < 0.01$, respectively). However, the expression of these two proteins in TGF-β1+ACE2 group was significantly reduced ($p < 0.001$ and $p < 0.01$, respectively) (Fig. 3G–I).

Inhibition of TGF-β1-Induced Epithelial-Mesenchymal Transition by ACE2

To investigate the suppressive impact of ACE2 on TGF-β1-induced epithelial-mesenchymal transition (EMT), the expression of proteins associated with EMT in

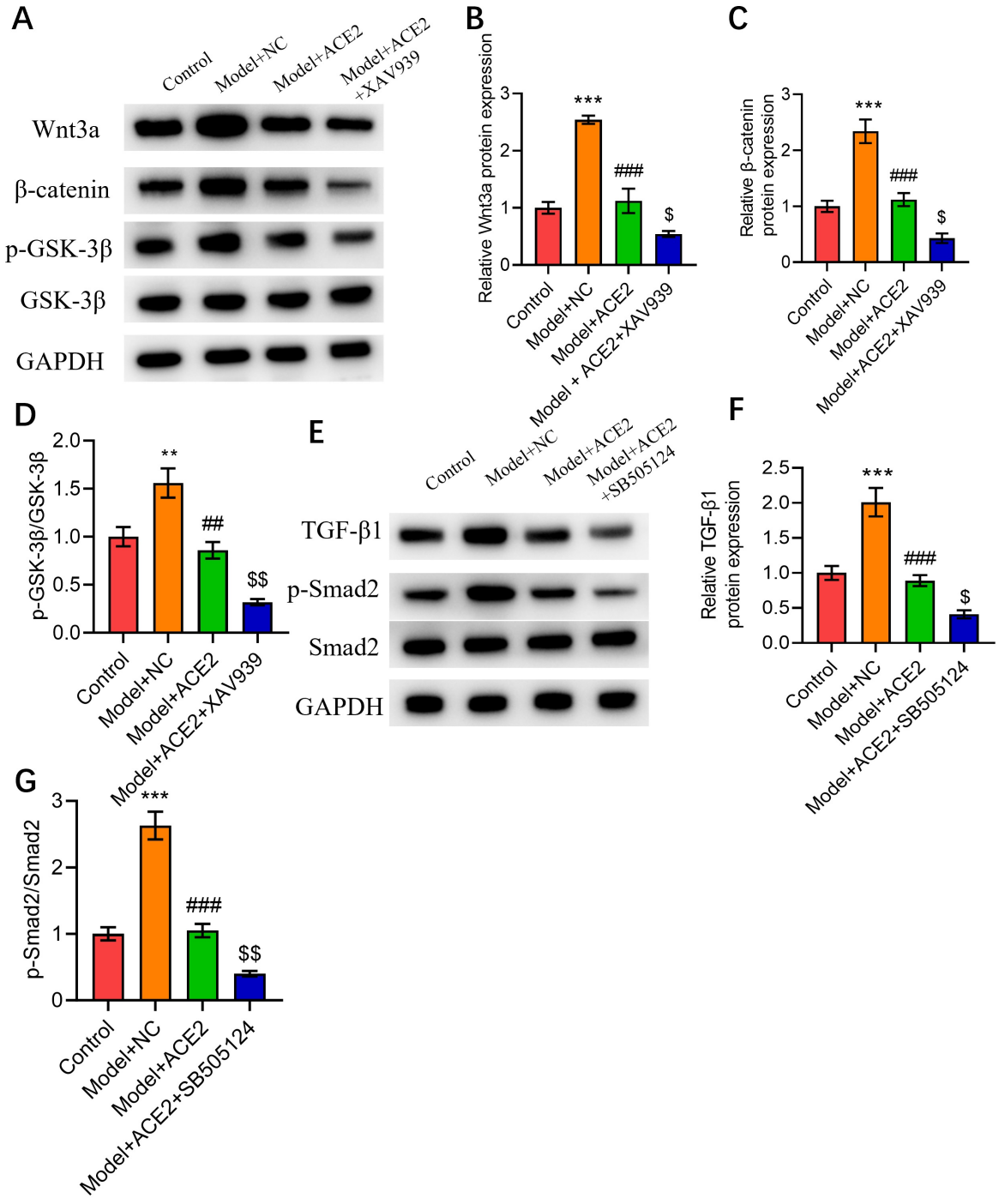

Fig. 2. The Wnt3a/β-catenin and transforming growth factor-β1 (TGF-β1)/Smad2 signaling pathways are affected by ACE2. (A–D) Protein levels related to the signaling pathways of Wnt3a, β-catenin, and p-GSK/GSK were analyzed using Western blotting. (E–G) Protein levels related to the signaling pathways of TGF-β1 and p-Smad2/Smad2 were analyzed using Western blotting. n = 6, $^{**}p < 0.01$, $^{***}p < 0.001$ compared to control group; $^{\#\#}p < 0.01$, $^{\#\#\#}p < 0.001$ compared to Model+NC group; $^{\$}p < 0.05$, $^{\$\$}p < 0.01$ compared to Model+ACE2 group. Wnt3a, Wnt Family Member 3a; GSK, glycogen synthase kinase; TGF-βRI, transforming growth factor-β type I receptor.

HLFs was analyzed. The TGF-β1 group exhibited the highest levels of vimentin and N-cadherin expression, but the lowest expression level of E-cadherin ($p < 0.001$ and $p < 0.01$, respectively). In contrast, the TGF-β1+ACE2 group exhibited decreased levels of vimentin and N-cadherin compared to the TGF-β1- group, whereas the expression of E-cadherin was elevated relative to the TGF-β1 group ($p < 0.001$ and $p < 0.01$, respectively) (Fig. 4A–C). Mor-

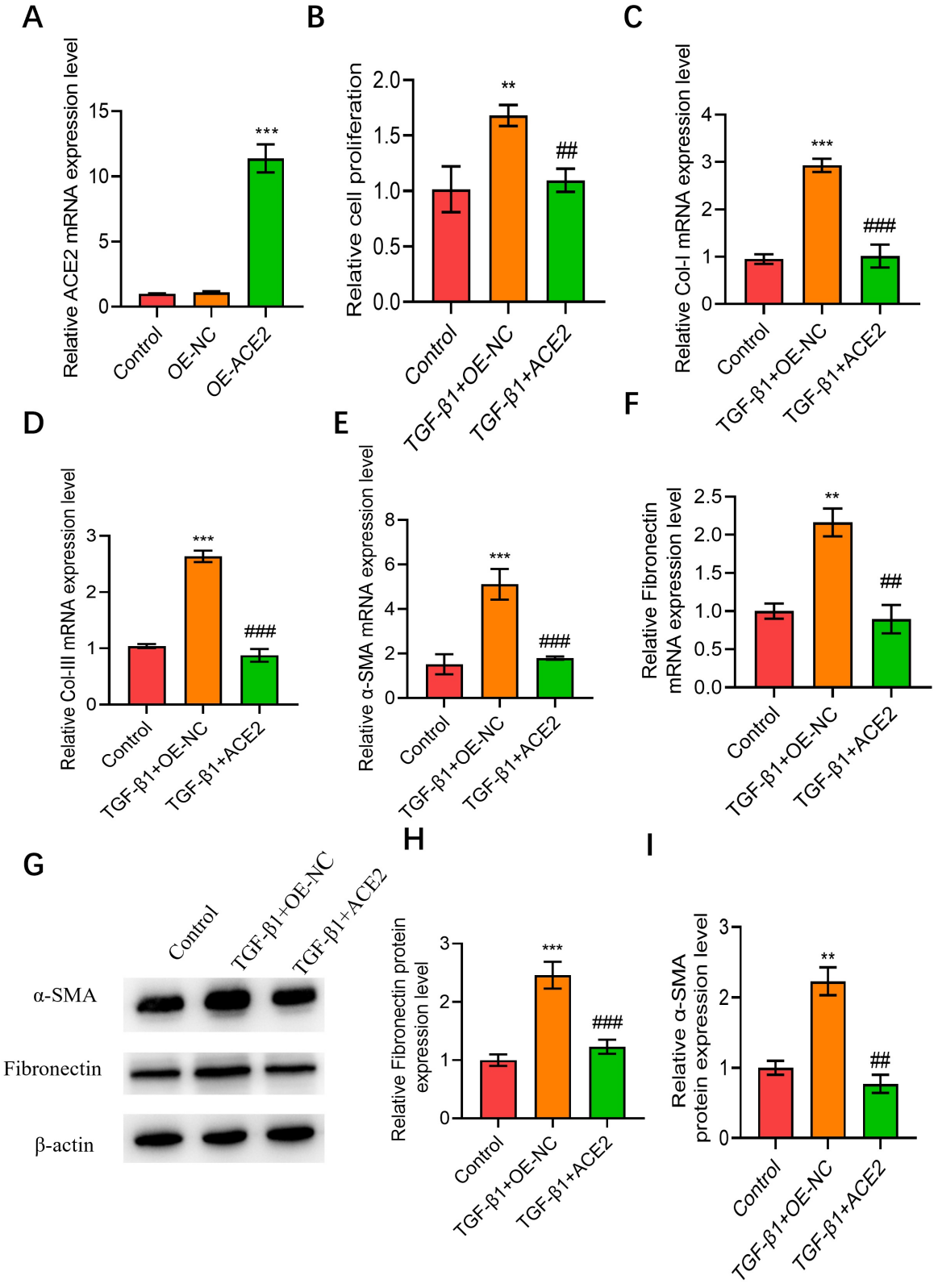

Fig. 3. Overexpression of ACE2 confers a protective effect against injury induced by TGF-β1 in human lung fibroblasts (HLFs). (A) mRNA expression levels of *ACE2* in HLFs. (B) The cell proliferation rate of treated HLFs was measured by 3-(4,5-Dimethylthiazol-2-yl)-2,5-diphenyltetrazolium bromide (MTT) assay. (C–F) Measurement of the mRNA expression of collagen I (*Col-I*), collagen III (*Col-III*), α-*SMA*, and fibronectin in HLFs. (G–I) Protein levels related to the signaling pathways of α-SMA and fibronectin were analyzed using Western blotting. n = 6. $^{**}p < 0.01$, $^{***}p < 0.001$ compared to control group; $^{\#\#}p < 0.01$, $^{\#\#\#}p < 0.001$ compared to TGF-β1+OE-NC group.

phological changes were observed in the TGF-β1 group, as evidenced by an increase in cell length ($p < 0.001$). In contrast, the cells in the TGF-β1+ACE2 group displayed reduced cell length, which was similar to that of the control group ($p < 0.01$) (Fig. 4D,E).

ACE2-Mediated Alleviation of TGF-β1-Induced Damage in Human Lung Fibroblasts

Western blot analysis was used to evaluate the impact of ACE2 on the Wnt/GSK-3β/β-catenin and TGF-β1/Smad2 signaling pathways in HLFs. Compared to the control group, the TGF-β1 group exhibited a notable increase in the protein expression levels of Wnt3a, β-catenin and p-GSK3β/GSK3β ($p < 0.001$ and $p < 0.01$, respectively), whereas the TGF-β1+ACE2 group exhibited a significant decrease in the ratio of p-GSK3β to GSK3β, and also a reduction in the protein levels of Wnt3a and β-catenin ($p < 0.001$, $p < 0.01$, $p < 0.05$, respectively) (Fig. 5A–D). In the TGF-β1 group, the levels of TGF-β1 and p-Smad2/Smad2 were elevated in comparison to the control group ($p < 0.05$). Nevertheless, in the TGF-β1+ACE2 group, the levels of TGF-β1 and p-Smad2/Smad resembled those of the control group (Fig. 5E–G). This implies that ACE2 mitigated the phosphorylation of GSK-3β and Smad2 that was enhanced by TGF-β1, thereby restoring their functionality.

Discussion

Pulmonary fibrosis is a pathological condition where an accumulation of collagen and excessive growth of connective tissue results in impaired lung function and respiratory distress [20,21]. ACE2 has gained significant interest in the past few years following the revelation of its involvement in the control of pulmonary fibrosis [22]. The current study discovered that ACE2 has a significant impact on reducing pulmonary fibrosis, in both *in vitro* and *in vivo* settings, associated with the Wnt/GSK-3β/β-catenin and TGF-β1/Smad2 signaling pathways.

Cellular damage and infiltration of inflammatory cells are consequences of inflammation, which is the initial event in pulmonary fibrosis [23]. Animal experiments demonstrated that overexpression of ACE2 can alleviate pathological inflammation in the lung tissue of mice. By inhibiting inflammatory responses and reducing pathological inflammation in lung tissue, ACE2 has the potential to halt the progression of pulmonary fibrosis. Studies suggested that pulmonary fibrosis is caused by the abnormal activation of the Wnt/GSK-3β/β-catenin signaling pathway, which is considered a critical mechanism [24,25]. Activation of the Wnt signaling pathway stabilizes β-catenin by inhibiting GSK-3β, thereby regulating the expression of genes related to cell proliferation and fibrosis. It has been shown that ACE2 can reduce the severity of pulmonary fibrosis by inhibiting the activation of the Wnt/GSK-3β/β-catenin signaling pathway [24,25]. Additionally, ACE2 may promote the degradation of β-catenin, thereby inhibiting the roles of both Wnt and TGF-β1 signaling pathways in fibrosis [10,24,25]. Smad2, as a downstream mediator of the TGF-β1 signaling cascade, promotes the expression of fibrotic genes and the production of extracellular matrix by activating Smad2/3 [26,27].

Furthermore, the benefits of ACE2 overexpression extend to ameliorating damage caused by TGF-β1 in HLFs and abrogating TGF-β1-induced EMT. EMT is a crucial process in pulmonary fibrosis, wherein epithelial cells transform into mesenchymal-like cells, leading to collagen deposition and connective tissue proliferation. The ability of ACE2 to inhibit TGF-β1-induced EMT is believed to contribute to its anti-fibrotic effects, thereby reducing the severity of pulmonary fibrosis. Our experimental results align with other studies [28–30], demonstrating that overexpression of ACE2 not only reduces pathological inflammation in lung tissue but also mitigates TGF-β1-induced damage in HLFs. Additionally, the anti-inflammatory properties of ACE2 play a crucial role in this regulatory network. We also demonstrated that ACE2 can attenuate the activity of Wnt/GSK-3β/β-catenin and TGF-β1/Smad2/3 signaling pathways by reducing the release of inflammatory mediators, illuminating a multifaceted mechanism for inhibiting fibrosis. This interplay suggests that ACE2 can comprehensively suppress the fibrotic process through multiple pathways, including inflammation, signal transduction, and cellular transformation. These results highlighted the importance of ACE2 in modulating the complex signaling network driving pulmonary fibrosis. Thus, a clearer understanding of these interactions may lead to the discovery of new molecular targets for therapeutic intervention and the development of ACE2-based treatment strategies.

The findings from this study underline the crucial involvement of ACE2 in controlling the Wnt/GSK-3β/β-catenin and TGF-β1/Smad2 signaling pathways, providing a fresh look at how ACE2 operates in pulmonary fibrosis. Additionally, our research confirms that ACE2 overexpression alleviates pulmonary fibrosis, presenting a novel target for therapeutic intervention. These insights into ACE2's regulatory role offer significant potential for clinical applications, particularly in developing targeted treatment strategies and improving patient management. By leveraging ACE2's ability to modulate key signaling pathways, new therapeutic approaches could be designed to specifically inhibit the progression of pulmonary fibrosis, thereby improving patient outcomes. For instance, ACE2-based therapies might be developed to reduce inflammation, prevent EMT, and promote the degradation of β-catenin, collectively contributing to the mitigation of fibrotic processes. Furthermore, the anti-inflammatory properties of ACE2 could be harnessed to address the underlying inflammatory responses that exacerbate fibrosis, potentially offering a multifaceted approach to treatment.

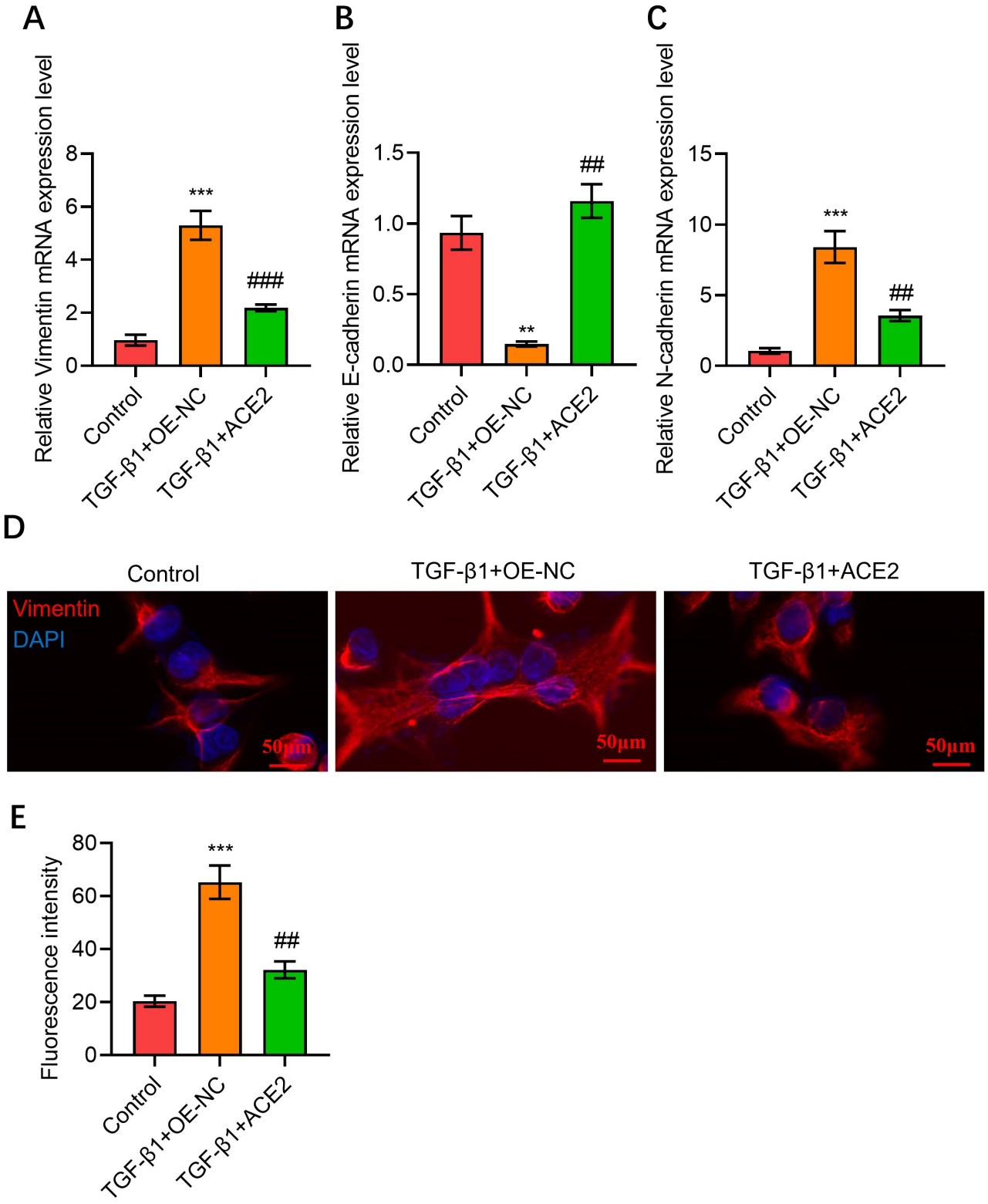

Fig. 4. ACE2 blocks the epithelial-mesenchymal transition (EMT) induced by TGF-β1. (A–C) mRNA expression levels of EMT-associated proteins such as vimentin, E-cadherin, and N-cadherin in human lung fibroblasts (HLFs). (D) Vimentin staining shows cellular morphological changes. Scale bar: 50 µm. (E) Relative fluorescence intensity quantified using Image J. n = 6. $^{**}p < 0.01$, $^{***}p < 0.001$ compared to control group; $^{\#\#}p < 0.01$, $^{\#\#\#}p < 0.001$ compared to TGF-β1+OE-NC group. DAPI, 4′,6-Diamidino-2′-phenylindole.

However, this study has certain limitations. A glaring limitation of the present study is we have yet to fully elucidate the mechanisms by which ACE2 operates in pulmonary fibrosis. Therefore, further detailed studies are re-

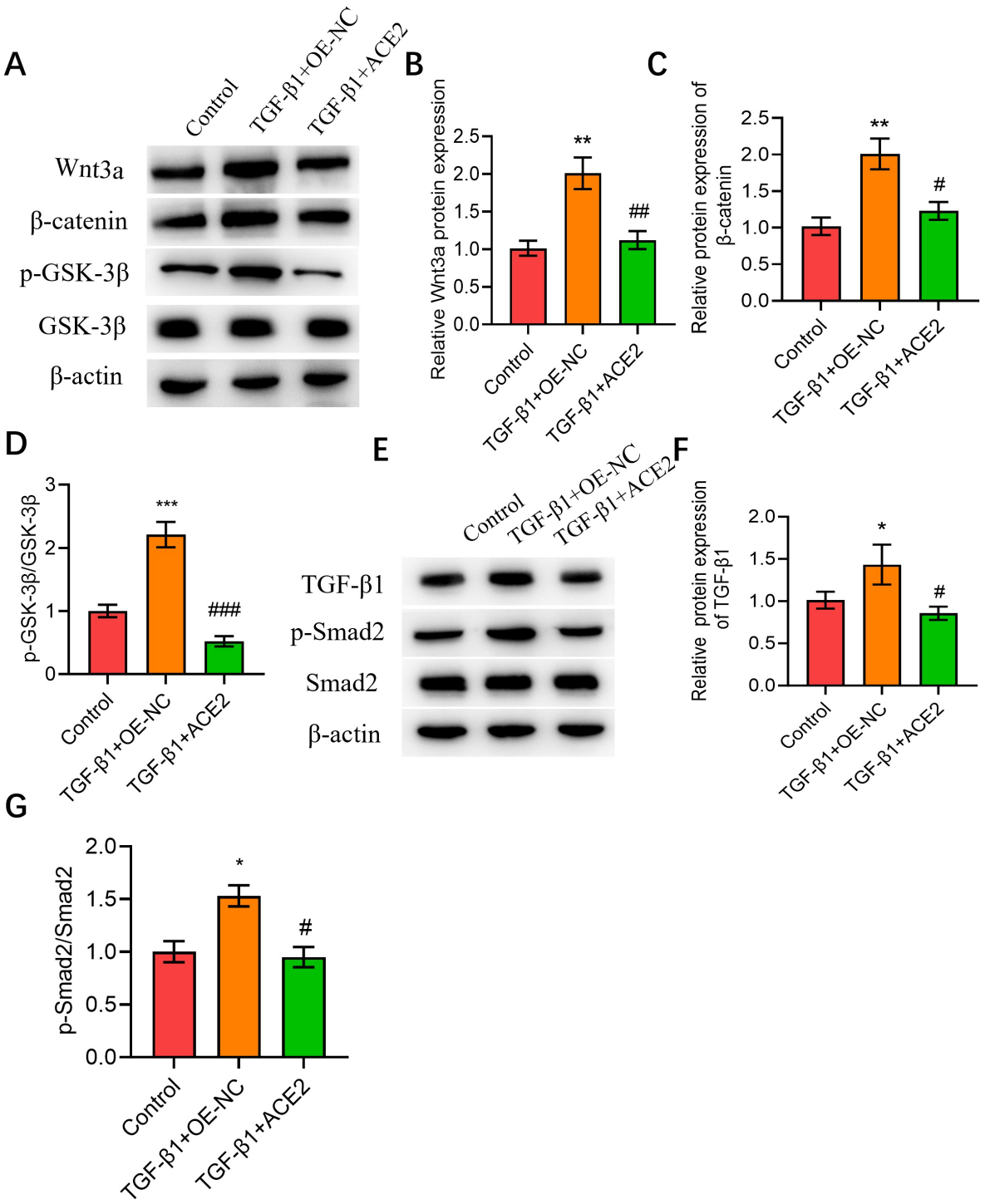

Fig. 5. ACE2 alleviates TGF-β1-induced damage in human lung fibroblasts (HLFs) related to the Wnt3a/β-catenin and TGF-β1/Smad2 signaling pathways. (A–D) Protein levels related to the signaling pathways of Wnt3a, β-catenin, and p-GSK/GSK were analyzed using Western blotting. (E–G) Protein levels related to the signaling pathways of TGF-β1 and p-Smad2/Smad2 were analyzed using Western blotting. n = 6. *$p < 0.05$, **$p < 0.01$, ***$p < 0.001$ compared to control group; $^{\#}p < 0.05$, $^{\#\#}p < 0.01$, $^{\#\#\#}p < 0.001$ compared to the TGF-β1+OE-NC group.

quired to delineate the exact molecular interactions and regulatory networks involving ACE2 in pulmonary fibrosis, in order to provide a complete picture of its comprehensive role. In addition, the present research primarily focuses on the short-term effects of ACE2 overexpression and does not fully capture the long-term implications and potential side effects of ACE2-based therapies. While our findings are promising, they are based on preclinical models, and

further validation in clinical trials is essential to determine the efficacy and safety of ACE2-targeted treatments in humans. Despite these limitations, our investigation not only advances a deeper understanding of pulmonary fibrosis but also highlights the potential of ACE2 as a therapeutic target, paving the way for innovative treatment strategies and improved patient care in clinical settings.

Conclusion

In summation, ACE2 holds promise in reducing lung fibrosis by controlling the Wnt/GSK-3β/β-catenin and TGF-β1/Smad2 signaling pathways. This study provides fresh optimism for enhancing the quality of life for patients and averting the development of pulmonary fibrosis. Additional investigations are warranted to enhance our comprehension regarding the mechanisms through which ACE2 functions in pulmonary fibrosis, with the aim of establishing a more robust theoretical foundation for advancing novel therapeutic approaches.

Availability of Data and Materials

The datasets used or analyzed during the present study are available from the corresponding author upon reasonable request.

Author Contributions

YT and JL designed the research study; LL performed the research; LL, YT and JL collected and analyzed the data. All authors have been involved in drafting the manuscript and all authors have been involved in revising it critically for important intellectual content. All authors have given final approval of the version to be published. All authors have participated sufficiently in the work to take public responsibility for appropriate portions of the content and agreed to be accountable for all aspects of the work in ensuring that questions related to its accuracy or integrity.

Ethics Approval and Consent to Participate

This study has been approved by the Institutional Animal Care and Use Committee of The First Hospital of Jiujiang City (No.20210421-03).

Acknowledgment

Not applicable.

Funding

This research received no external funding.

Conflict of Interest

The authors declare no conflict of interest.

References

[1] Spagnolo P, Kropski JA, Jones MG, Lee JS, Rossi G, Karampitsakos T, *et al*. Idiopathic pulmonary fibrosis: Disease mechanisms and drug development. Pharmacology & Therapeutics. 2021; 222: 107798.

[2] Moss BJ, Ryter SW, Rosas IO. Pathogenic Mechanisms Underlying Idiopathic Pulmonary Fibrosis. Annual Review of Pathology. 2022; 17: 515–546.

[3] Raghu G, Remy-Jardin M, Richeldi L, Thomson CC, Inoue Y, Johkoh T, *et al*. Idiopathic Pulmonary Fibrosis (an Update) and Progressive Pulmonary Fibrosis in Adults: An Official ATS/ERS/JRS/ALAT Clinical Practice Guideline. American Journal of Respiratory and Critical Care Medicine. 2022; 205: e18–e47.

[4] Maher TM, Bendstrup E, Dron L, Langley J, Smith G, Khalid JM, *et al*. Global incidence and prevalence of idiopathic pulmonary fibrosis. Respiratory Research. 2021; 22: 197.

[5] Karampitsakos T, Juan-Guardela BM, Tzouvelekis A, Herazo-Maya JD. Precision medicine advances in idiopathic pulmonary fibrosis. EBioMedicine. 2023; 95: 104766.

[6] Lv Q, Wang J, Xu C, Huang X, Ruan Z, Dai Y. Pirfenidone alleviates pulmonary fibrosis in vitro and in vivo through regulating Wnt/GSK-3β/β-catenin and TGF-β1/Smad2/3 signaling pathways. Molecular Medicine (Cambridge, Mass.). 2020; 26: 49.

[7] Yi J, Pan J, Zhang S, Mao W, Wang J, Wang W, *et al*. Jiedu Huoxue decoction improves chronic abacterial prostatitis/chronic pelvic pain syndrome through activating Wnt/GSKβ/β-catenin signaling pathway and alleviating apoptosis. Biomedicine & Pharmacotherapy. 2022; 149: 112830.

[8] Tu M, Wei T, Jia Y, Wang Y, Wu J. Molecular mechanisms of alveolar epithelial cell senescence and idiopathic pulmonary fibrosis: a narrative review. Journal of Thoracic Disease. 2023; 15: 186–203.

[9] Kang L, Wang X, Wang J, Guo J, Zhang W, Lei R. NRF1 knockdown alleviates lipopolysaccharide-induced pulmonary inflammatory injury by upregulating DKK3 and inhibiting the GSK-3β/β-catenin pathway. Clinical and Experimental Immunology. 2023; 214: 120–129.

[10] Morganstein T, Haidar Z, Trivlidis J, Azuelos I, Huang MJ, Eidelman DH, *et al*. Involvement of the ACE2/Ang-(1-7)/MasR Axis in Pulmonary Fibrosis: Implications for COVID-19. International Journal of Molecular Sciences. 2021; 22: 12955.

[11] Wang Q, Zhang Y, Wu L, Niu S, Song C, Zhang Z, *et al*. Structural and Functional Basis of SARS-CoV-2 Entry by Using Human ACE2. Cell. 2020; 181: 894–904.e9.

[12] Lan J, Ge J, Yu J, Shan S, Zhou H, Fan S, *et al*. Structure of the SARS-CoV-2 spike receptor-binding domain bound to the ACE2 receptor. Nature. 2020; 581: 215–220.

[13] Narula S, Yusuf S, Chong M, Ramasundarahettige C, Rangarajan S, Bangdiwala SI, *et al*. Plasma ACE2 and risk of death or cardiometabolic diseases: a case-cohort analysis. Lancet (London, England). 2020; 396: 968–976.

[14] Gupta D, Kumar A, Mandloi A, Shenoy V. Renin angiotensin aldosterone system in pulmonary fibrosis: Pathogenesis to therapeutic possibilities. Pharmacological Research. 2021; 174: 105924.

[15] Lu W, Eapen MS, Singhera GK, Markos J, Haug G, Chia C, *et al*. Angiotensin-Converting Enzyme 2 (ACE2), Transmembrane Peptidase Serine 2 (TMPRSS2), and Furin Expression Increases in the Lungs of Patients with Idiopathic Pulmonary Fibrosis (IPF) and Lymphangioleiomyomatosis (LAM): Implications for SARS-CoV-2 (COVID-19) Infections. Journal of Clinical Medicine. 2022; 11: 777.

[16] Lin X, Lin W, Zhuang Y, Gao F. Angiotensin-Converting

Enzyme 2 Inhibits Lipopolysaccharide-Caused Lung Fibrosis via Downregulating the Transforming Growth Factor β-1/Smad2/Smad3 Pathway. The Journal of Pharmacology and Experimental Therapeutics. 2022; 381: 236–246.

[17] Guo J, Wei X, Li Q, Li L, Yang Z, Shi Y, *et al*. Single-cell RNA analysis on ACE2 expression provides insights into SARS-CoV-2 potential entry into the bloodstream and heart injury. Journal of Cellular Physiology. 2020; 235: 9884–9894.

[18] Li S, Li Y, Xu H, Wei Z, Yang Y, Jin F, *et al*. ACE2 Attenuates Epithelial-Mesenchymal Transition in MLE-12 Cells Induced by Silica. Drug Design, Development and Therapy. 2020; 14: 1547–1559.

[19] Ronca RD, Myers AM, Ganea D, Tuma RF, Walker EA, Ward SJ. A selective cannabinoid CB2 agonist attenuates damage and improves memory retention following stroke in mice. Life Sciences. 2015; 138: 72–77.

[20] Phan THG, Paliogiannis P, Nasrallah GK, Giordo R, Eid AH, Fois AG, *et al*. Emerging cellular and molecular determinants of idiopathic pulmonary fibrosis. Cellular and Molecular Life Sciences: CMLS. 2021; 78: 2031–2057.

[21] Somogyi V, Chaudhuri N, Torrisi SE, Kahn N, Müller V, Kreuter M. The therapy of idiopathic pulmonary fibrosis: what is next? European Respiratory Review: an Official Journal of the European Respiratory Society. 2019; 28: 190021.

[22] Huang WJ, Tang XX. Virus infection induced pulmonary fibrosis. Journal of Translational Medicine. 2021; 19: 496.

[23] Glass DS, Grossfeld D, Renna HA, Agarwala P, Spiegler P, DeLeon J, *et al*. Idiopathic pulmonary fibrosis: Current and future treatment. The Clinical Respiratory Journal. 2022; 16: 84–96.

[24] Shenoy V, Qi Y, Gupta D, Katovich M, Raizada M. Small moleculae ACE2 activator, diminazene aceturate attenuates bleomycin-induced pulmonary fibrosis. European Respiratory Journal. 2012; 40: P1765.

[25] Huang G, Zhang J, Qing G, Liu D, Wang X, Chen Y, *et al*. *S100A2* Silencing Relieves Epithelial-Mesenchymal Transition in Pulmonary Fibrosis by Inhibiting the Wnt/β-Catenin Signaling Pathway. DNA and Cell Biology. 2021; 40: 18–25.

[26] Cui Y, Xin H, Tao Y, Mei L, Wang Z. Arenaria kansuensis attenuates pulmonary fibrosis in mice via the activation of Nrf2 pathway and the inhibition of NF-kB/TGF-beta1/Smad2/3 pathway. Phytotherapy Research: PTR. 2021; 35: 974–986.

[27] Jia L, Sun P, Gao H, Shen J, Gao Y, Meng C, *et al*. Mangiferin attenuates bleomycin-induced pulmonary fibrosis in mice through inhibiting TLR4/p65 and TGF-β1/Smad2/3 pathway. The Journal of Pharmacy and Pharmacology. 2019; 71: 1017–1028.

[28] Xue T, Wei N, Xin Z, Qingyu X. Angiotensin-converting enzyme-2 overexpression attenuates inflammation in rat model of chronic obstructive pulmonary disease. Inhalation Toxicology. 2014; 26: 14–22.

[29] Ye R, Liu Z. ACE2 exhibits protective effects against LPS-induced acute lung injury in mice by inhibiting the LPS-TLR4 pathway. Experimental and Molecular Pathology. 2020; 113: 104350.

[30] Jia H. Pulmonary Angiotensin-Converting Enzyme 2 (ACE2) and Inflammatory Lung Disease. Shock (Augusta, Ga.). 2016; 46: 239–248.